J|A|C|S
ARTICLES
Published on Web 01/18/2002

Quantitative Measurements of Recombinant HIV Surface Glycoprotein 120 Binding to Several Glycosphingolipids Expressed in Planar Supported Lipid Bilayers

John C. Conboy,[†] Katherine D. McReynolds,[‡] Jacquelyn Gervay-Hague,*[,§] and S. Scott Saavedra*

Contribution from the Department of Chemistry, University of Arizona, Tucson, Arizona 85721-0041

Received May 17, 2001

Abstract: The interaction of recombinant HIV-1 surface glycoprotein gp120 (rgp120) with natural isolates of lactosylceramide (LacCer), glucosylceramide (GlcCer), and galactosylceramide (GalCer) has been quantitatively measured under equilibrium conditions using total internal reflection fluorescence (TIRF) spectroscopy. The binding affinity (K_a) of rgp120 to these glycosphingolipids (GSLs), reconstituted at 5 mol % in supported planar lipid bilayers composed of 95 mol % POPC, is ca. 10^6 M^{-1} for dissolved rgp120 concentrations greater than 25 nM. In contrast, at concentrations of rgp120 between 0.2 and 15 nM, rgp120 does not bind significantly to LacCer and GlcCer, but has a high affinity for GalCer with a measured K_a value of 1.6×10^9 M^{-1}. However, protein surface coverage measurements show that this strong binding process accounts for very little of the total protein adsorbed over the entire concentration range studied. At a protein concentration of ca. 20 nM, the surface coverage is only 3% of that achieved at apparent saturation (i.e., when the protein concentration is ca. 220 nM). Thus the "high affinity" binding sites comprise only a small fraction of the total number of binding sites. Several other variables were investigated. Rgp120 binding behavior at membranes doped with α-hydroxygalactosylceramide (α-GalCer) was very similar to that observed with GalCer, showing that the presence/absence of an α-hydroxy moiety does not significantly affect galactosylceramide recognition. Phase segregation of GalCer, which occurs when the mole fraction of this GSL in a POPC bilayer exceeds ca. 0.1, was also investigated and showed no effect on binding affinity at low rgp120 concentrations. To investigate the influence of fatty acid chain length, GSLs with monodisperse C_{18} and C_{24} chain lengths, both with and without an α-hydroxy moiety, were synthesized, and their binding affinity to rgp120 was examined. Relative to the natural isolates (which contain a mixture of chain lengths), minimal differences were observed; thus among the compounds tested, fatty acid chain length does not affect GSL recognition. The results of this work should aid efforts to design anti-HIV-1 agents based on membrane-tethered, carbohydrate-based receptors for rgp120.

Introduction

The HIV virus gains entry into host cells through a cascade of events mediated by the viral glycoproteins gp120 and gp41.[1] Gp120 is a surface protein, noncovalently bound to the transmembrane protein gp41. Together these two glycoproteins are presented in trimeric form on the viral surface.[2] HIV is known to infect host cells expressing both a critical domain protein called CD4 and chemokine co-receptors such as CXCR4 and CCR5.[3] T-lymphocytes and macrophages are the primary targets of HIV infection, and the process is initiated by interactions between gp120, CD4, and the chemokine co-receptor. These interactions lead to conformational changes in gp120, which subsequently unmask a hydrophobic region of gp41 that is capable of inserting into the host cell membrane. Trimeric gp41 is a six-helix bundle comprised of three carboxy terminal peptides linked to three amino-terminal peptides via loop regions.[4] In the native state of gp41, the C and N peptides are believed to be in an extended form. Once gp41 is unmasked and the fusion domain has been inserted into the host membrane, the C-peptides associate with the N-peptides forming a hairpin structure.[2] This event brings the host-cell and viral membranes into close proximity allowing viral entry into host cells.

Current chemotherapeutic interventions of HIV infection are directed toward inhibiting enzymes that are required for viral

* To whom correspondence should be addressed. S.S.S.: voice, 520-621-9761; fax, 520-621-8407; e-mail, saavedra@u.arizona.edu.
[†] Current address: Department of Chemistry, University of Utah, 315 S. 1400 E., Salt Lake City, UT 84112.
[‡] Current address: Department of Chemistry, California State University, Sacramento, 6000 J. Street, Sacramento, CA 95819.
[§] Current address: Department of Chemistry, University of California, Davis, One Shields Avenue, Davis, CA 95616.

(1) (a) Allan, J. S.; Coligan, J. E.; Barin, F.; McLane, M. F.; Sodroski, J. G.; Rosen, C. A.; Haseltine, W. A.; Lee, T. H.; Essex, M. *Science* **1985**, *228*, 1091−1094. (b) Barin, F.; McLane, M. F.; Allan, J. S.; Lee, T. H.; Groopman, J. E.; Essex, M. *Science* **1985**, *228*, 1094−1096. (c) McKeating, J. A.; Willey, R. L. *AIDS* **1989**, *3*, S35−S41.
(2) (a) Chan, D. C.; Kim, P. S. *Cell* **1998**, *93*, 681−84. (b) Eckert, D. M.; Kim, P. S. *Annu. Rev. Biochem.* **2001**, *70*, 777−810.
(3) Littman, D. R. *Cell* **1998**, *93*, 677−80 and references therein.
(4) (a) Chan, D. C.; Fass, D.; Berger, J. M.; Kim, P. S. *Cell* **1997**, *89*, 263−273. (b) Weissenhorn, W.; Dessen, A.; Harrison, S. C.; Skehel, J. J.; Wiley, D. C. *Nature* **1997**, *387*, 426−430.

10.1021/ja011225s CCC: $22.00

replication, once a host cell has been invaded. Typically a combination of HIV reverse transcriptase and protease inhibitors is prescribed in what is known as highly active anti-retroviral therapy (HAART).[5] However, the emergence of viral strains that are resistant to these drugs has fueled investigations into alternative intervention strategies. One active area of research has focused on preventing HIV entry into host cells. Recent developments in the production of fusion inhibitors are particularly promising. Peptide-derived compounds have been shown to block association of the C- and N-termini of gp41 preventing formation of the hairpin structure.[6]

We have concentrated our efforts on an earlier step in the entry process in an effort to block gp120 interactions with cellular receptors, which would effectively cap gp41 and prohibit normal fusion events. Galactosyl ceramide (GalCer (**1**)) is a glycosphingolipid (GSL) expressed on mucosal membrane cells that do not express CD4. Several studies have shown that an alternative pathway of HIV infection occurs in these CD4 cells through gp120 interactions with GalCer.[7−11] The GalCer binding site is distinct from the region on gp120 that recognizes CD4, which presents the opportunity for targeted drug delivery.[12] We have proposed that synthetic compounds, capable of binding to the GalCer site, could be used to deliver a second ligand that blocks CD4 and chemokine co-receptor interactions. Understanding the molecular events that are responsible for HIV recognition of GalCer is a critical step in developing this dual ligand approach to preventing HIV entry into host cells.

Literature on the affinity of gp120 for GalCer and related GSLs is surprisingly inconsistent. Harouse et al.[8,9] and Bhat et al.[13] used high performance thin-layer chromatography (HPTLC) and enzyme-linked immunosorbent assays (ELISA) to determine the binding of several GSLs to recombinant gp120 (rgp120). GalCer (**1**), glucosylceramide (GlcCer (**2**)), lactosylceramide (LacCer (**3**)), psychosine (**4**)), and ceramide (Cer (**5**)) were compared, and only GalCer and psychosine were bound by rgp120 (see structures in Figure 1). Latov and co-workers used immunospot assays on nitrocellulose and thin-layer chromatography plates as well as ELISA to test the binding affinity of

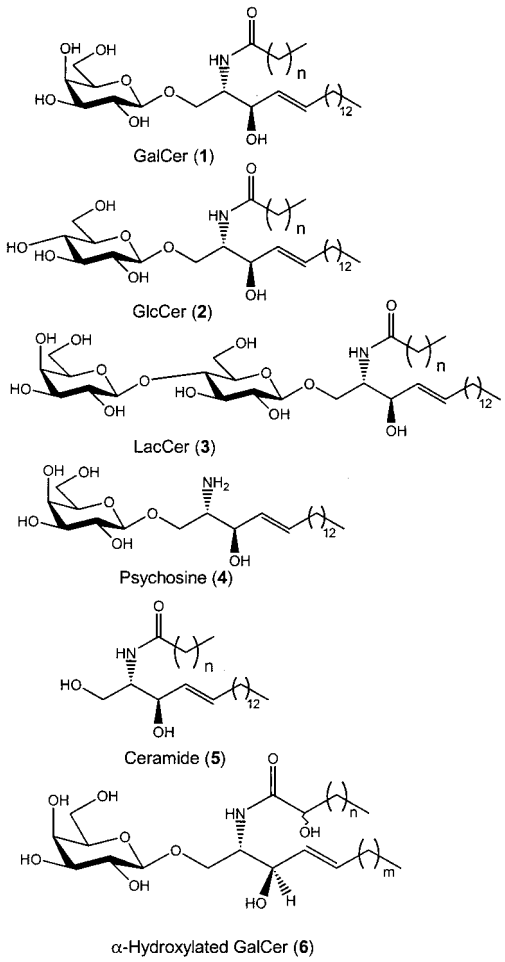

Figure 1. Structures of galactosyl ceramide (GalCer, **1**), glucosyl ceramide (GlcCer, **2**), lactosyl ceramide (LacCer, **3**), psychosine (**4**), ceramide (Cer, **5**), and α-hydroxy galactosyl ceramide (α-GalCer, **6**).

rgp120 for GalCer.[10] Only the immunospot assay on TLC indicated that gp120 recognized GalCer. Long et al.[14] studied interactions of rgp120 and liposomes doped with mixtures of phosphatidylethanolamine, phosphatidylcholine, cholesterol, and various glycolipids (GalCer, GlcCer, LacCer, psychosine). They reported that rgp120 strongly bound liposomes containing GalCer, while GlcCer and LacCer were bound less efficiently, and psychosine was inactive. More recently, McReynolds et al.[15] reported results from a biotin-NeutrAvidin adhesion assay, which showed that rgp120 has similar binding affinities for GalCer, GlcCer, and LacCer.

The assays used to study gp120/GSL interactions have inherent limitations that may explain the aforementioned anomalies. Conventional, heterogeneous solid-phase assays (e.g., an ELISA or TLC method) pose problems since proper geometric presentation of membrane-bound receptors in a bioactive conformation is not always possible. The presentation problem can be overcome using a liposome-flotation[14] or a cell-based immunofluorescence assay,[10] but it is difficult to obtain a complete binding curve (i.e., from very low surface coverage to saturation) using these methods. Furthermore, none of these methods can provide a quantitative measurement of the binding

(5) Stephenson, J. *J. Am. Med. Assoc.* **1999**, *282*, 1317−18.
(6) (a) Jiang, S.; Lin, K.; Strick, N.; Neurath, A. R. *Nature* **1993**, *365*, 113. (b) Wild, C. T.; Shugars, D. C.; Greenwall, T. K.; McDanal, C. B.; Mathews, T. J. *Proc. Natl. Acad. Sci. U.S.A.* **1994**, *91*, 9770−9774. (c) Furuta, R. A.; Wild, C. T.; Weng, T.; Weiss, C. D. *Nat. Struct. Biol.* **1998**, *5*, 276−279. (d) Rimsky, L. T.; Shugars, D. C.; Mathews, T. J. *J. Virol.* **1998**, *72*, 986−993. (e) Judice, J. K.; Tom, J. Y.; Huang, W.; Wrin, T.; Vennari, J.; Petropoulos, C. J.; McDowell, R. S. *Proc. Natl. Acad. Sci. U.S.A.* **1997**, *94*, 13426−30.
(7) Yahi, N.; Baghdiguian, S.; Moreau, H.; Fantini, J. *J. Virol.* **1992**, *66*, 4848−4854.
(8) Harouse, J. M.; Kunsch, C.; Hartle, H. T.; Laughlin, M. A.; Hoxie, J. A.; Wigdahl, B.; Gonzalezscarano, F. *J. Virol.* **1989**, *63*, 2527−2533.
(9) Harouse, J. M.; Bhat, S.; Spitalnik, S. L.; Laughlin, M.; Stefano, K.; Silberberg, D. H.; Gonzalezscarano, F. *Science* **1991**, *253*, 320−323.
(10) McAlarney, T.; Apostolski, S.; Lederman, S.; Latov, N. *J. Neurosci. Res.* **1994**, *37*, 453−460.
(11) (a) Brogi, A.; Presentini, R.; Solazzo, D.; Piomboni, P.; Constantinoccecarini, E. *AIDS Res. Hum. Retroviruses* **1996**, *12*, 483−489. (b) Brogi, A.; Presentini, R.; Piomboni, P.; Collodel, G.; Strazza, M.; Solazzo, D.; Costantinoceccarini, E. *J. Submicrosc. Cytol. Pathol.* **1995**, *27*, 565−571.
(12) (a) Bhat, S.; Mettus, R. V.; Reddy, E. P.; Ugen, K. E.; Srikanthan, V.; Williams, W. V.; Weiner, D. B. *AIDS Res. Hum. Retroviruses* **1993**, *9*, 175. (b) Fantini, J.; Hammache, D.; Delézay, Yahi, N.; André-Barres, C.; Rico-Lattes, O.; Lattes, A. *J. Biol. Chem.* **1997**, *272*, 7245. (c) Speck, R. F.; Wehrly, K.; Platt, E. J.; Atchison, R. E.; Charo, I. F.; Kabat, D.; Chesebro, B.; Goldsmith, M. A. *J. Virol.* **1997**, *71*, 7136−7139. (d) Olshevsky, U.; Helseth, E.; Furman, C.; Li, J.; Haseltine, W.; Sodroski, J. *J. Virol.* **1990**, *64*, 5701−5707.
(13) Bhat, S.; Spitalnik, S. L.; Gonzalezscarano, F.; Silberberg, D. H. *Proc. Natl. Acad. Sci. U.S.A.* **1991**, *88*, 7131−7134.
(14) Long, D.; Berson, J. F.; Cook, D. G.; Doms, R. W. *J. Virol.* **1994**, *68*, 5890−5898.
(15) McReynolds, K. D.; Hadd, M. J.; Gervay-Hague, J. *Bioconjugate Chem.* **1999**, *10*, 1021.

affinity at equilibrium, which makes comparisons of binding data problematic.

To overcome these limitations, we have implemented total internal reflection fluorescence (TIRF) spectroscopy to study rgp120 binding to a series of GSLs. TIRF spectroscopy is a well-established technique for the quantitative study of protein interfacial behavior.[16−22] By labeling the protein with a fluorophore, protein adsorption and desorption kinetics, lateral and rotational diffusion processes, and membrane-induced structural changes have been investigated. Furthermore, exciting the sample in a TIR geometry confines the incident light to the near-surface region of the sample which significantly reduces the contribution of bulk (dissolved) protein to the measured signal.[20] Since it is not necessary to remove the aqueous protein solution in contact with the membrane prior to making a measurement, receptor−ligand binding processes can be studied under equilibrium conditions. TIRF, in combination with methods to deposit supported phospholipid bilayers[23,24] on planar optical substrates, allows a diverse array of behaviors at model membrane surfaces to be examined. In addition, a planar supported lipid bilayer more closely approximates a cellular surface as compared to a unilamellar vesicle, which has a high radius of curvature. Consequently, TIRF microscopy at the surface of a planar supported bilayer overcomes some of the limitations of the previous methods used to study gp120−GSL binding.

We recently reported the use of TIRF to measure equilibrium binding affinities of rgp120 to natural isolates of GalCer, GlcCer, and LacCer.[25] In this paper, we extend those studies to include α-hydroxy GalCer (**6**) (Figure 1). In addition to determining protein-GSL affinity constants, a modified form of a TIRF quantitation method has been used to determine the relative surface coverages of rgp120 bound to GSL-bearing membranes. Several physical parameters that may affect rgp120 binding behavior have also been investigated, including (i) the effect of concentration-dependent phase segregation of GSLs when incorporated into a fluid lipid bilayer,[14] and (ii) the effect of the length of the fatty acid chain in a GSL[25] on rgp120 recognition.

Experimental Section

Materials. The FITC-rgp120 (IIIB) purchased from Intracel was the full-length, glycosylated protein obtained from the baculovirus expression system. According to the commercial supplier,[26] (i) the protein purity was >90% as estimated by Coomassie blue stained gel, (ii) the protein was recognized by anti-gp120 MAB in ELISA and Western Blot assays, and (iii) the protein reacted with anti-gp120 antibodies from human serum in Dot Blot. The fluorescein labeling density was determined by absorbance and fluorescence spectroscopy to be 3.8 ± 1.2 FITC:rgp120. FITC conjugated streptavidin (Pierce) with a labeling ratio of 2.9:1 was used for nonspecific protein adsorption studies.

1-Palmitoyl-2-oleoylphosphatidylcholine (POPC) was purchased from Avanti Polar lipids. Fluorescein isothiocyanate (FITC) labeled phosphoethanolamine (FITC-PE) and FITC conjugated dextran (10 000 MW, 2.2:1 FITC:dextran) were purchased from Molecular Probes. The naturally occurring GSLs (structures shown in Figure 1) lactosylceramide (LacCer) (bovine), glucosylceramide (GlcCer) (Gaucher's spleen), and ceramide (Cer) were purchased from Matreya. Galactosylcermaide (GalCer) (bovine, Type I) and α-hydroxy galactosylceramide (α-GalCer) (bovine, Type II) were purchased from Sigma. The commercially available GSLs were natural isolates and therefore contained saturated and unsaturated fatty acid chains ranging from C_{16}−C_{24} and were not hydroxylated except in the case of α-GalCer.[27] All commercially obtained lipids were used without further purification

Preparation of Synthetic GSLs. To investigate the influence of fatty acid chain length and α-hydroxylation on rgp120/GSL recognition, several GSLs having monodisperse fatty acid chains were synthesized. Two analogues of α-hydroxy GalCer, β-D-galactopyranosyl-(1 → 1)-2-*N*-(2-hydroxy-stearamide)-sphingenine (α-GalCer-C_{18}) (**7a**) and β-D-galactopyranosyl-(1 → 1)-2-*N*-(2-hydroxy-tetracosamide)-sphingenine (α-GalCer-C_{24}) (**7b**), were prepared according to Scheme 1. Briefly, the α-hydroxy fatty acid (**8** or **9**) was acetylated prior to activation with tetrafluorophenyl trifluoroacetate. The activated acid was condensed with psychosine and subsequently deacetylated with sodium methoxide to afford the desired products **7a**/**b**. The corresponding analogues of GalCer, β-D-galactopyranosyl-(1 → 1)-2-*N*-stearamide-sphingenine (GalCer-C_{18}) (**20**) and β-D-galactopyranosyl-(1 → 1)-2-*N*-tetracosamide-sphingenine (GalCer-C_{24}) (**21**), were prepared according to Scheme 2. Briefly, the fatty acid (**16** or **17**) was first activated with tetrafluorophenyl trifluoroacetate. The intermediate was then condensed with psychosine to afford the desired products **20** and **21**. A detailed description of the synthesis of all four products (**20**, **21**, **7a**/**b**) is presented in the Supporting Information.

Preparation of Planar Membrane Substrates. Planar supported lipid bilayers (PSLBs) used in TIRF adsorption assays were prepared on fused silica slides (4 × 2.5 cm, Dynasil). The fused silica substrates were first sonicated in 50% isopropyl alcohol/50% water (v/v), rinsed in Nano-Pure water with a measured resistivity of 18 MΩ cm, treated with 30% H_2O_2/70% concentrated H_2SO_4 for 30 min, and then rinsed repeatedly in Nano-Pure water. PSLBs doped with GSLs used in binding assays were deposited using the Langmuir−Blodgett−Schaefer technique.[28] The bilayers were asymmetric in that GSLs were present only in the outer lipid monolayer (i.e., the monolayer in contact with the overlying aqueous solution). The inner monolayer of the PSLB (i.e., the monolayer in contact with the fused silica substrate) was composed of pure POPC. GSLs were incorporated into the outer monolayer of the PSLB at molar ratios of 20:1 and 1:1 POPC:GSL. Monolayers were transferred to the substrate at a surface pressure of 35 mN/m, corresponding to 58 Å^2/molecule. Nano-Pure water was used as the subphase. All depositions were carried out at 25 °C. After formation, PSLBs were maintained in an aqueous environment at all times.

Protein Adsorption Studies. A micro-TIRF flow cell (volume of ca. 50 μL) was constructed to minimize the amount of rgp120 needed to perform binding studies. A schematic of the cell is shown in Figure 2. The cell consists of a Viton O-ring held in place above a quartz slide by a Teflon block. Two 0.5 mm diameter holes on either side of the block allow for insertion of a syringe needle to introduce solutions into the volume above the fused silica substrate. The light coupling arrangement of the cell consists of two right-angle quartz prisms. One

(16) Burmeister, J. S.; Olivier, L. A.; Reichert, W. M.; Truskey, G. A. *Biomaterials* **1998**, *19*, 307−325.
(17) Kalb, E.; Engel, J.; Tamm, L. K. *Biochemistry* **1990**, *29*, 1607−1613.
(18) Thompson, N. L.; Poglitsch, C. L.; Timbs, M. M.; Pisarchick, M. L. *Acc. Chem. Res.* **1993**, *26*, 568−573.
(19) Pisarchick, M. L.; Thompson, N. L. *Biophys. J.* **1990**, *58*, 1235−1249.
(20) Hlady, V.; Reinecke, D. R.; Andrade, J. D. *J. Colloid Interface Sci.* **1986**, *111*, 555−569.
(21) Pisarchick, M. L.; Gesty, D.; Thompson, N. L. *Biophys. J.* **1992**, *63*, 215−223.
(22) Timbs, M. M.; Poglitsch, C. L.; Pisarchick, M. L.; Sumner, M. T.; Thompson, N. L. *Biochim. Biophys. Acta* **1991**, *1064*, 219−228.
(23) Tamm, L. K.; McConnell, H. M. *Biophys. J.* **1985**, *47*, 105−113.
(24) Thompson, N. L.; Palmer, A. G., III. *Mol. Cell. Biophys.* **1988**, *5*, 39−56.
(25) Conboy, J. C.; McReynolds, K. D.; Gervay-Hague, J.; Saavedra, S. S. *Angew. Chem., Int. Ed.* **2000**, *39*, 2882−2884.
(26) (a) Technical Bulletin for Catalog #12003, Intracel Corp., 8/14/1996. (b) Intracel Retroviral Products Catalog, 1998; p 11.
(27) Technical Bulletin #131303, Avanti Polar Lipids, Inc.
(28) McConnell, H. M.; Watts, T. H.; Weis, R. M. *Biochim. Biophys. Acta* **1984**, *864*, 95−106.

Scheme 1

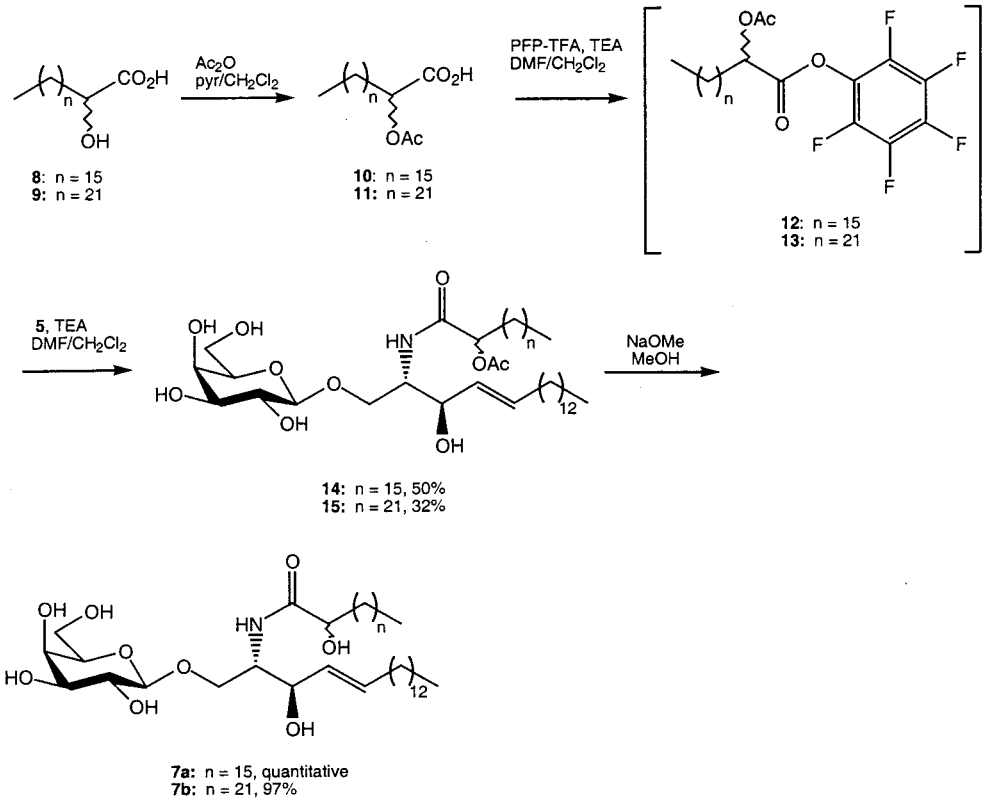

Scheme 2

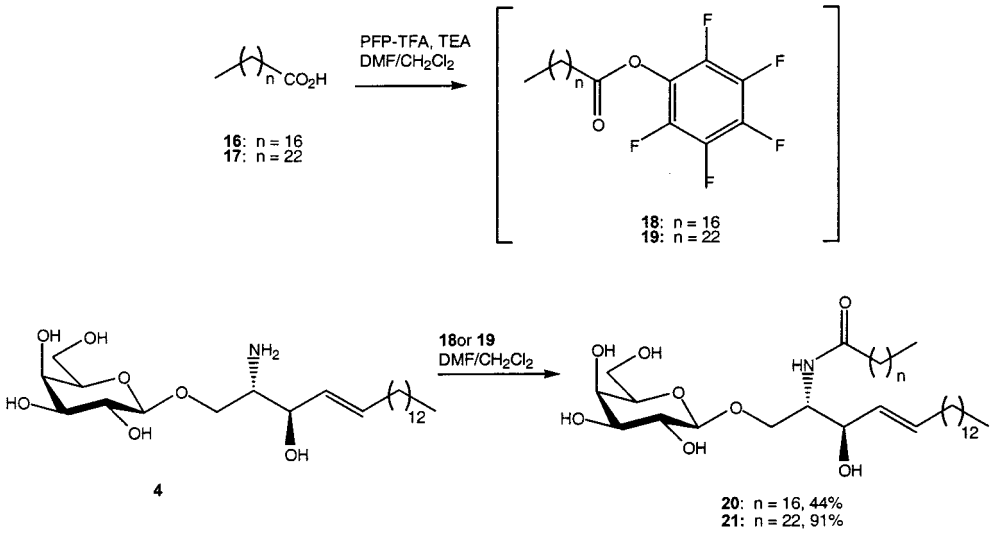

prism is used to couple the excitation light (488 nm from an argon ion laser) into the fused silica slide. After propagating down the length of the slide by total internal reflection, the second prism is used to outcouple the beam, thereby reducing scattered light in the cell volume. Index matching fluid (1.458 n_d, Cargille) was used for efficient in- and outcoupling of the laser light.

Increasing concentrations of FITC-rgp120 in 150 mM phosphate buffered saline (50 mM phosphate) were injected into the flow cell and allowed to equilibrate with the surface for 30 min prior to each measurement, which was determined experimentally to be a sufficient time for a steady-state response to be observed. The flow cell was mounted on a Nikon Diaphot inverted microscope. Fluorescence emission was back-collected through the quartz slide with a 4× objective, optically filtered with a 514 nm long-pass filter, and detected with a photomultiplier tube. The incident excitation light at 488 nm was modulated at a frequency of 2.5 kHz. Phase sensitive detection was used to retrieve the fluorescence intensity. The experiment was interfaced to a PC using Lab Windows for data collection. All experiments were performed at 25 °C.

Determination of Binding Affinities. Two different models were used to extract the equilibrium binding constants from the fluorescence data: (i) a conventional Langmuir model which assumes no cooperativity (i.e., the affinity of each binding site is identical); (ii) a Langmuir-like model that includes a cooperative process, in which the binding of FITC-rgp120 to the ligand-bearing membrane promotes subsequent binding of additional rgp120 molecules.[29] The Langmuir model used had the following form:

$$[\mathrm{rgp120}]K_a = \frac{F}{F_{max} - F} \quad (1)$$

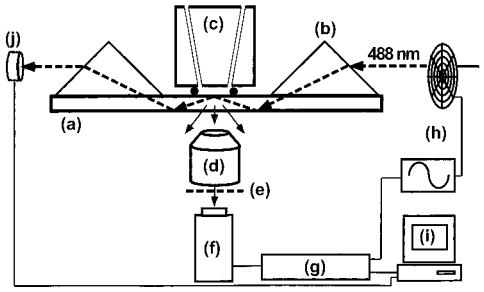

Figure 2. Schematic of the micro-TIRF cell and associated instrumental components: (a) fused silica slide, (b) quartz prism, (c) Teflon block and Viton O-ring, (d) 4× microscope objective, (e) 510 nm long pass filter, (f) PMT, (g) lock-in amplifier, (h) frequency generator, (i) data acquisition computer, and (j) reference photodiode.

where F_{max} is the maximum fluorescence intensity at surface saturation, F is the fluorescence intensity measured as a function of the bulk rgp120 concentration, [rgp120], and K_a is the equilibrium binding constant. The cooperative Langmuir model used was of the following form:

$$\omega^{(F/F_{max})}[\text{rgp120}]K_a = \frac{F}{F_{max} - F} \tag{2}$$

where ω is an additional term to account for surface bound protein−protein interactions. A derivation of eq 2 is given in ref 29. For values of $\omega < 1$ the interaction is noncooperative, and for $\omega > 1$ the interaction is cooperative. When $\omega = 1$, eq 2 reverts to eq 1 (no protein−protein interaction). Depending on the observed binding behavior, the fluorescence data were fit to eq 1 using the fitting parameters of F_{max} and K_a, or to eq 2 using the fitting parameters F_{max}, K_a, and ω. An iterative solution was obtained by nonlinear regression using SigmaPlot. In both cases, it was assumed that the activity coefficient of rgp120 is unity. However, this assumption may not be valid if rgp120 self-association occurs over the concentration range examined (note that gp120 self-associates in vivo[2]). With respect to GSLs, the Langmuir model assumes unity activity, but this assumption may not be valid when the GSLs comprise a significant mole fraction of the lipids in the upper leaflet of a PSLB. In contrast, the cooperative model allows for a distribution of binding site activities. Such a distribution could arise, for example, from GSL self-association (i.e., lipid rafting[30]) in a PSLB. Some of these issues are discussed in more detail below.

Fluorescence Calibration. The relative surface coverage of rgp120 adsorbed to PSLBs was determined by calibration of the measured fluorescence intensity. Since the measured fluorescence intensity is directly proportional to the adsorption cross section and the fluorescence quantum yield of the FITC label on rgp120, it is possible to determine the interfacial concentration of adsorbed protein species.[20,31] The fluorescence intensity measured in TIRF geometry can be expressed as

$$I_F = \phi d_e \epsilon I_o c \int_0^\infty e^{-2z/d_p}\,dz \tag{3}$$

where ϕ is the fluorescence quantum yield, d_e is the detector efficiency, ϵ is the extinction coefficient, c is the concentration, I_o is the incident intensity, and the integral represents the decay of the evanescent field in the rarer medium[32] with a characteristic penetration depth of d_p, which is given by the following equation:

$$d_p = \frac{\lambda}{2\pi n_1\left[\left(\sin^2\theta - \frac{n_2}{n_1}\right)\right]^{1/2}} \tag{4}$$

The fluorescence measured from adsorbed FITC-rgp120 at equilibrium is the sum of the fluorescence from the adsorbed protein and the fluorescence from the dissolved protein in the near surface region. The total fluorescence intensity from the surface (F_s) can be expressed as

$$F_s = \phi_s d_e \epsilon I_o \frac{\Gamma_{rgp120}}{\Delta}\int_0^\Delta e^{-2z/d_p}\,dz + \phi_b d_e \epsilon I_o c_{rgp120}\int_\Delta^\infty e^{-2z/d_p}\,dz \tag{5}$$

where Δ is the thickness of the protein layer (a thickness of 93 Å was used for the adsorbed rgp120 layer − see below), Γ_{rgp120} is the surface concentration of rgp120, and ϕ_s and ϕ_b are the quantum efficiencies of FITC at the surface and in the bulk solution, respectively. At low concentrations (less than 10^{-7} M), the solution contribution to the total fluorescence (right side of eq 5) is minimal and can be ignored. Equation 5 can be used to determine the surface density of adsorbed protein if the values of ϕ_s, d_e, and I_o are known. In the absence of direct knowledge of these values, the quantity of adsorbed protein can be determined empirically by calibration of the measured fluorescence intensity.

Calibration was performed by measuring the fluorescence from several standard solutions of FITC-labeled dextran introduced above the substrate surface. Prior to the injection of the standards, the surface was first "washed" with a 1% solution of Triton X-100 to remove the supported lipid bilayer and adsorbed FITC-rgp120. This procedure provided a "clean" background to measure the evanescently excited FITC-dextran fluorescence and precluded nonspecific interactions of the dextran with the protein-coated surface. The evanescently excited solution fluorescence (F_b) is expressed by

$$F_b = \phi_b d_e \epsilon I_o c_{dextran}\int_0^\infty e^{-2z/d_p}\,dz \tag{6}$$

where the limits of integration describe the extent of the evanescent field as it decays in the rarer aqueous medium. By taking the ratio of the measured fluorescence from the adsorbed FITC-rgp120 (eq 5) and the FITC-dextran solution (eq 6), the following expression is obtained:

$$\frac{F_s}{F_b} = \frac{\phi_{sf} d_e \epsilon I_o \Gamma_{rgp120}\int_0^\Delta e^{-2z/d_p}\,dz}{\phi_{blk} d_e \epsilon I_o \Delta c_{dextran}\int_0^\infty e^{-2z/d_p}\,dz} \tag{7}$$

The assumption is made that the quantum yield of FITC conjugated to rgp120 is identical to that of FITC conjugated to dissolved dextran, that is, $\phi_s/\phi_b \approx 1$. Equation 7 then reduces to the following:

$$\frac{F_s}{F_b} = \frac{\Gamma_{rgp120}\int_0^\Delta e^{-2z/d_p}\,dz}{\Delta c_{dextran}\int_0^\infty e^{-2z/d_p}\,dz} \tag{8}$$

A plot of measured fluorescence intensity versus the bulk concentration of the FITC-dextran standards yields the proportionality constant necessary to calculate the surface coverage of rgp120.

Results and Discussion

Binding Affinity of Rgp120 to Natural GSLs. Representative adsorption isotherms of FITC-rgp120 binding to LacCer, GlcCer, GalCer, and Cer doped at 5 mol % into the outer leaflet of a PSLB are plotted in Figure 3 over the entire concentration range (0.2−220 nM) of dissolved rgp120 that was studied. Also displayed is the binding curve for FITC-rgp120 incubated with

(29) Zhao, S. L.; Walker, D. S.; Reichert, W. M. *Langmuir* **1993**, *9*, 3166−3173.
(30) (a) Simons, K.; Ikonen, E. Functional Rafts in Cell Membranes. *Nature* **1997**, *387*, 569−572. (b) Dietrich, C.; Bagatolli, L. A.; Volovyk, Z. N.; Thompson, N. L.; Levi, M.; Jacobson, K.; Gratton, E. Lipid Rafts Reconstituted in Model Membranes. *Biophys. J.* **2001**, *80*, 1417−1428.
(31) (a) Rebar, V. A.; Santore, M. M. *Macromolecules* **1996**, *29*, 6262−6272. (b) Shibata, C. T.; Lenhoff, A. M. *J. Colloid Interface Sci.* **1992**, *148*, 469.
(32) Harrick, N. J. *Internal Reflection Spectroscopy*; Interscience: New York, 1967.

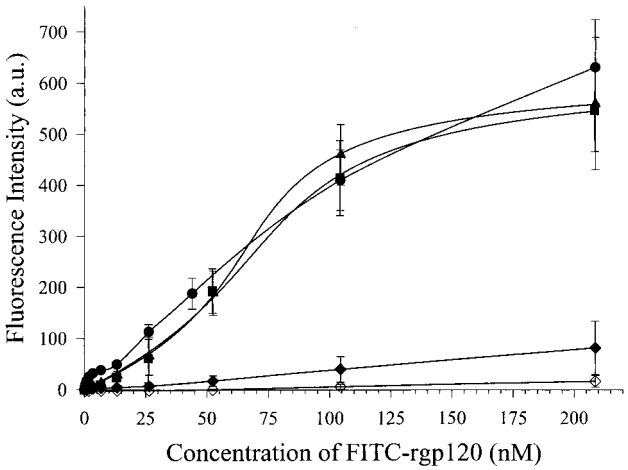

Figure 3. TIRF adsorption isotherms of FITC-rgp120 adsorption to POPC membranes doped with 5 mol % GalCer (●), GlcCer (■), LacCer (▲), Cer (◆), and to a pure POPC membrane (◇). The data plotted represent the average of three independent measurements for each sample. The solid lines through the data of GlcCer and LacCer represent fits to the data using a cooperative Langmuir isotherm. For GalCer, the sum of two independent Langmuir isotherms was used to fit the data. The solid lines through the data for Cer and POPC are shown as a guide to the eye only.

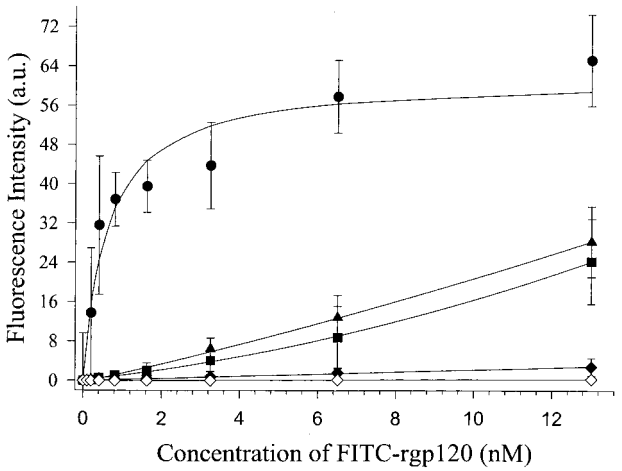

Figure 4. TIRF adsorption isotherms of FITC-rgp120 adsorption at low protein concentrations (0−15 nM) to POPC membranes doped with 5 mol % GalCer (●), GlcCer (■), LacCer (▲), Cer (◆), and to a pure POPC membrane (◇). The data plotted represent the average of three independent measurements for each sample. The solid lines through the data of GlcCer and LacCer represent fits to the data using a cooperative Langmuir isotherm. A single Langmuir isotherm was used to fit the GalCer data. The solid lines through the data for Cer and POPC are shown only as a guide to the eye.

a pure POPC bilayer. The fluorescence intensities plotted in Figure 3 are normalized relative to the intensity measured for a standard solution of FITC-dextran, which was introduced into the cell after measurements for each binding curve were completed. The fluorescence intensities plotted in Figure 3 can therefore be compared directly.

A comparison of the binding curves shows that there is only minimal nonspecific interaction of rgp120 with a pure POPC bilayer. Rgp120 adsorption to a Cer-doped bilayer, which lacks the terminal sugar group, is comparable to that observed for rgp120 to POPC. In contrast, considerable protein adsorption occurs at bilayers doped with LacCer, GlcCer, and GalCer. Thus glycosylation of the lipid appears to be crucial to rgp120 recognition and binding, as has been observed by a number of other researchers.[13,14,33] An additional, negative control was performed using FITC-streptavidin. Adsorption of this protein to a membrane doped with 5 mol % GalCer was minor (i.e., comparable to streptavidin adsorption to pure POPC membrane; data not shown). A protein lacking a carbohydrate recognition site therefore exhibits minimal nonspecific adsorption to a GSL-bearing PSLB.

The TIRF isotherms for binding to PSLBs bearing LacCer, GlcCer, and GalCer are very similar in the protein concentration range of 25−220 nM (Figure 3). However, a closer examination of the data at concentrations of dissolved rgp120 less than 25 nM reveals differences in binding behavior among these three GSLs. In Figure 4, the data presented in Figure 3 are replotted over the protein concentration range of 0.2−15 nM. Rgp120 exhibits a high affinity for a GalCer-doped bilayer in this concentration regime. In contrast, PSLBs doped with LacCer and GlcCer show only a small, linear increase in protein adsorption when dissolved rgp120 is less than 15 nM. Similar to the behavior observed in the high concentration regime, there is no significant rgp120 interaction with either pure POPC or Cer-doped bilayers.

Table 1. Summary of Binding Constants and Surface Coverages for Rgp120 Binding to Planar POPC Membranes Doped with Various GSLs

	low rgp120 concentration (0.2–15 nM)		high rgp120 concentration (25–220 nM)	
GSL	K_a (M^{-1}) × 10^9	Γ (mol/cm²) × 10^{-14} [a]	K_a (M^{-1}) × 10^6	Γ (mol/cm²) × 10^{-14} [a]
GalCer (**1**)	1.6 ± 0.9	0.15 ± 0.05	7.5 ± 3.2	5.7 ± 0.9
α-GalCer (**6**)	0.31 ± 0.12	0.30 ± 0.08	4.6 ± 1.3	5.0 ± 1.1
GlcCer (**2**)			3.8 ± 1.1[b]	3.1 ± 0.7
LacCer (**3**)			3.6 ± 2.1[b]	3.1 ± 0.8
ceramide (**5**)		0.014 ± 0.003		0.40 ± 0.05
POPC (no GSL)		0.001 ± 0.0006		0.10 ± 0.01
GalCer-C_{18} (**20**)	1.2 ± 0.5	0.20 ± 0.06		
GalCer-C_{24} (**21**)	1.1 ± 0.3	0.14 ± 0.02		
α-GalCer-C_{18} (**7a**)	0.37 ± 0.6			
α-GalCer-C_{24} (**7b**)	0.28 ± 0.1			

[a] Surface coverages were calculated at the apparent saturation level (F_{max} in eqs 1 and 2) in each concentration range. [b] For GlcCer- and LacCer-doped membranes, K_a was recovered by fitting the isotherm data to a cooperative model (eq 2) over the entire rgp120 concentration range studied (0.2−220 nM).

The equilibrium constants for rgp120 binding to the various GSLs in PSLBs were extracted by fitting the TIRF isotherms to either a Langmuir (eq 1) or a cooperative binding (eq 2) model. The recovered binding constants are summarized in Table 1. A satisfactory fit to the adsorption data for LacCer- and GlcCer-doped membranes over the entire rgp120 concentration range studied (0.2−220 nM) was achieved only when a cooperative model was used. In these cases, we observed binding behavior that was qualitatively very similar to that reported by Zhao and Reichert[29] for streptavidin binding to biotinylated lipids in a PSLB. F-tests were performed to statistically compare fitting the data to both models.[34] The null hypothesis was that the Langmuir model adequately described the data. The resulting p-values of 1.6×10^{-6} and 2.7×10^{-4} for GlcCer and LacCer

(33) Delezay, O.; Yahi, N.; Fantini, J. *Perspect. Drug Discovery Des.* **1996**, *5*, 192−202.

(34) Abramowitz, M.; Stegun, L. A. *Handbook of Mathematical Functions*; Dover: New York, 1965; p 299.

provide strong evidence that the observed binding behavior is cooperative rather than Langmuir-like.

The binding constants (K_a) recovered using the cooperative model are 3.6×10^6 and 3.8×10^6 M^{-1} for LacCer and GlcCer, respectively. The corresponding interaction constants (ω) are 2.0 and 1.8, respectively. For $\omega > 1$ the binding process is considered cooperative in nature, which means that the surface free energy increases with the addition of rgp120 to the membrane surface, thereby promoting the adsorption of additional protein molecules. This explains the minimal protein adsorption observed at low dissolved concentrations of rgp120 and subsequent sharp increase at higher protein concentrations.

For rgp120 adsorption to GalCer-doped membranes, the adsorption process was fit using a sum of two independent Langmuir isotherms (eq 1). In other words, the binding data obtained at low dissolved rgp120 concentrations (0.2−15 nM) and at high dissolved concentrations (25−220 nM) were treated independently. This assumption is reasonable since (i) there is a difference of 3 orders of magnitude between the K_a values for two binding processes (Table 1), and (ii) the binding process in the low concentration regime (<20 nM) undergoes apparent saturation (Figure 4) and therefore does not contribute significantly to the protein adsorption process at concentrations greater than 25 nM.

In the region of high dissolved rgp120 concentration (25−220 nM), the recovered K_a value is 7.5×10^6 M^{-1}. Although this value is slightly greater than that observed for LacCer and GlcCer in the same concentration range, it does not represent a statistically significant difference. At low concentrations of dissolved rgp120 (<20 nM), GalCer is clearly the preferred receptor, relative to LacCer and GlcCer, with a recovered K_a of 1.6×10^9 M^{-1}. Although the GalCer adsorption data are modeled here as two discrete binding events, the possibility that cooperative rgp120 binding occurs, as observed for LacCer and GlcCer, cannot be eliminated. The initial, high affinity binding of rgp120 to GalCer may serve to stimulate further protein adsorption at higher concentrations. This explanation is consistent with the similar binding behavior observed at high concentrations of dissolved rgp120 for all three GSLs. The strong binding event at low rgp120 concentrations is what differentiates the activity of GalCer from LacCer and GlcCer.

The rgp120−GSL binding affinities measured here, most notably for GalCer, are unusually high for proteins and their carbohydrate ligands; comparable binding constants have been reported for the interaction between gp120 and its natural protein target, the CD4 receptor.[39] However, the observation of a strong binding event between GalCer and rgp120 is consistent with data obtained by Long et al. using a liposome flotation assay.[14] An additional comparison can be obtained by quantitative analysis of the surface tension data reported by Hammache et al.[35] for the adsorption of rgp120 to a monolayer of α-GalCer at the air−water interface. Using a differential form of the Gibbs adsorption equation and assuming Langmuir binding, a binding constant of 2.1×10^9 is obtained,[36] which is comparable to the results reported herein. Unusually strong binding between proteins and carbohydrates has also been reported for other ligand−receptor pairs. Bewley and Otero-Quintero measured nanomolar binding constants for polyvalent interactions between cyanovirin-N and mannose-containing oligomers.[37] Other examples, discussed in two recent reviews,[38] illustrate how both preorganized protein−protein complexes and clustered carbohydrate ligands can produce protein−carbohydrate binding affinities in the micro- and nanomolar regimes. However, at this time the mechanism responsible for the strong rgp120−GSL binding observed herein is not known. On the basis of the literature in this area,[14,35−38] multivalent binding is the most probable explanation. Aggregation of GSLs into microdomains (i.e., lipid rafts[30]) could promote multivalent interactions (however, see below). Protein−protein binding is an additional consideration, given that gp120 is presented as a trimer on the surface of HIV.[2] Initial binding of rgp120 molecules to GSLs at the surface of a PSLB could promote additional, thermodynamically enhanced protein adsorption due to rgp120 self-recognition; this mechanism would explain the cooperative binding behavior described above.

Rgp120 Surface Coverage on Planar Membranes Bearing Natural GSLs. A modification of the TIRF calibration method first described by Hlady et al.[20] was used to determine the surface coverage (Γ) of rgp120 adsorbed to PSLBs doped with GSLs. Surface coverages were calculated at the apparent saturation level in each of the two dissolved rgp120 concentration regimes studied: the low regime (0.2−15 nM) and the high regime (25−220 nM). When expressed in fluorescence intensity units, the apparent saturation level refers to the parameter F_{max} in eqs 1 and 2. Implementing the TIRF calibration method allowed the recovered F_{max} values to be converted to Γ values, which are listed in Table 1.

Before discussing these data, it is important to note that use of the TIRF calibration method to determine the *absolute* surface coverage of an adsorbed protein film can be problematic. As discussed previously by a number of authors,[20,31] there are several contributing factors that may yield an inaccurate Γ value: (1) Self-quenching of FITC fluorescence, due to energy transfer, may occur when FITC-labeled protein molecules are

(35) Hammache, D.; Pieroni, G.; Yahi, N.; Delezay, O.; Koch, N.; Lafont, H.; Tamalet, C.; Fantini, J. *J. Biol. Chem.* **1998**, *273*, 7967−7971.

(36) Analysis of the surface pressure data published by Hammache et al.[35] was done using the differential form of the Gibbs adsorption equation,

$$\Gamma_{gp120} = \frac{1}{2RT}\left(\frac{\partial \pi}{\partial \ln(a_{rgp120})}\right)_T$$

where Γ_{rgp120} is the surface excess of rgp120, π is the surface pressure, and a is the activity of rgp120. For the dilute solutions used in the work of Hammache, the activity has been replaced with the subphase concentration. Assuming a Langmuir adsorption process, an integral form of the surface pressure as a function bulk concentration can be derived,

$$\pi = \Gamma_{max} 2RT \ln(1 + K_a c_{gp120})$$

where Γ_{max} is the maximum surface excess, and K_a is the affinity constant. A satisfactory fit to the surface tension data with a calculated association constant of 9.8×10^9 M^{-1} and a surface coverage of approximately 0.22×10^{-12} mol/cm^2 at saturation was extracted from the data. Note: Errors in the measured surface pressure, the choice of an appropriate isotherm model, and the relatively few number of experimental data points can result in errors of greater than 40% for the calculated surface densities and binding affinities.

(37) Bewley, C. A.; Otero-Quintero, S. *J. Am. Chem. Soc.* **2001**, *123*, 3892−3902.

(38) (a) Lee, R. T.; Lee, Y. C. *Glycoconjugate J.* **2001**, *17*, 543−551. (b) Mammen, M.; Choi, S.-K.; Whitesides, G. M. *Angew. Chem., Int. Ed.* **1998**, *37*, 2754−2794.

(39) An affinity constant of $K_a = 7.7 \times 10^8$ M^{-1} for rgp120 binding to intact, solubilized radioiodinated CD4 was measured by saturation binding analysis (Lundin, K.; Nygren, A.; Arthur, L. O.; Robey, W. G.; Morein, B.; Ramstedt, U.; Gidlund, M.; Wigzell, H. *J. Immunol. Methods* **1987**, *97*, 93−100). In the case of rgp120 binding to CD4 on whole cells, a $K_a = 2.5 \times 10^8$ M^{-1} was measured (Smith, D. H.; Byrn, R. A.; Marsters, S. A.; Gregory, T.; Groopman, J. E.; Capon, D. J. *Science* **1987**, *238*, 1704−1707). Thus the strength of rgp120−GalCer association at a POPC membrane is clearly comparable to that of the initial binding event in the primary HIV infection pathway.

closely packed in an adsorbed film. In this case, the ratio ϕ_s/ϕ_b (in eq 7) will be significantly less than 1, and systematically low Γ values will result. (2) In the TIRF geometry, excitation of a fluorophore can occur via either evanescent or scattered radiation.[20,31] The ratio of evanescent- to scatter-excited emission varies depending on the distance of the fluorophore from the interface where TIR occurs. Since FITC-dextran calibration solution occupies the entire evanescent volume, whereas the FITC-rgp120 film occupies only the near-surface region, the ratio of evanescent- to scatter-excited emission generated from the standards and the film will be quite different. This problem will also produce systematically low Γ values. **(**3) A film thickness (Δ in eq 8) of 93 Å has been assumed for the adsorbed protein layer. This value is based on a calculated hydrodynamic radius of 46 Å for rgp120, which was estimated empirically from dynamic light scattering data for globular proteins of various size.[40] However, if the shape of rgp120 is not spherical, or if rgp120 molecules undergo conformational changes upon adsorption, the protein layer thickness may be significantly different from the assumed value, which may yield an inaccurate determination of Γ.

Because of these limitations, surface coverage measurements determined using the TIRF calibration are predicted to be systematically underestimated.[41] Thus we cannot, for example, determine the stoichiometry of rgp120−GSL binding. However, the results from measurements on different films can still be quantitatively compared, since they are highly accurate on a *relative* basis. Thus we turn to a comparison of relative Γ values (listed in Table 1) determined for rgp120 adsorbed to 5 mol % GalCer, LacCer, GlcCer, Cer, and POPC PSLBs. The highest surface coverage, 5.7×10^{-14} mol/cm^2, is found for GalCer in the high rgp120 concentration regime. On Cer-doped and pure POPC membranes, the respective Γ values of 0.40×10^{-14} and 0.10×10^{-14} mol/cm^2 are less than 10% of that measured for GalCer. Thus the level of nonspecific protein adsorption to GSL-bearing membranes appears to be insignificant. At LacCer- and GlcCer-bearing membranes, equal coverages of 3.1×10^{-14} mol/cm^2 were found. This Γ value is about 60% of the coverage observed for GalCer, which is consistent with the binding affinity measurements at high rgp120 concentrations, showing that GalCer is the preferred receptor.

In the low rgp120 concentration regime, nonspecific adsorption also accounts for less than 10% of the protein adsorption to a GalCer-doped membrane, based on a comparison of the Γ values determined for GalCer-doped (0.15×10^{-14} mol/cm^2), Cer-doped (0.014×10^{-14} mol/cm^2), and pure POPC (0.001×10^{-14} mol/cm^2) membranes. (Note: Surface coverages were not determined for LacCer- and GlcCer-doped membranes, due to the minimal binding observed at low rgp120 concentrations.)

A more significant result is that the GalCer surface coverage is 0.15×10^{-14} mol/cm^2, which accounts for only a small fraction of the surface coverage achieved at saturation in the high concentration regime. Thus, despite the fact that the binding of rgp120 to GalCer is very strong ($K_a = 1.6 \times 10^9$ M^{-1}) at protein concentrations <20 nM, this event produces a low protein surface coverage. If we assume that two classes of rgp120 binding sites exist on a GalCer-doped membrane, the high affinity sites account for only ca. 3% of the total sites, with the balance of ca. 97% being "low" affinity" sites. Consequently, at a dissolved rgp120 concentration of ca. 220 nM, almost all of the adsorbed protein molecules are bound by a relatively weak (and likely different) mechanism than that which is responsible for adsorption of the strongly bound fraction.

The physical basis for the existence of two classes of binding sites is not clear at this time. As discussed above, one possibility is that multivalent, high affinity binding occurs at GSL microdomains (i.e., lipid rafts[30]), and lower affinity binding occurs at regions on the PSLB where the GSLs are more spatially dispersed. However, the experimental evidence acquired to date (see below) does not definitively support (or refute) this hypothesis. Regardless, it is clear that the two-site behavior is what distinguishes rgp120 binding at a GalCer-bearing membrane from rgp120 binding at membranes doped with LacCer and GlcCer. Finally, the structural basis for preferential recognition of GalCer is also unclear at this time, and it will probably remain unclear until the structure of the GSL binding site on gp120 is determined.

Effect of α-Hydroxylation of GalCer on Rgp120 Recognition. Several previous investigations have suggested that the structure of the fatty acid chain of GalCer can modulate the binding of this molecule to gp120. In particular, Hammache et al.[35] suggested that α-hydroxylation of the fatty acid chain is required for gp120 recognition, since only minimal binding was observed when the fatty acid was not α-hydroxylated. This suggests that the hydroxy moiety is involved in gp120 recognition of GalCer. However, the TIRF adsorption data presented in Figures 3 and 4 and in Table 1 for GalCer, which lacks the α-hydroxy group, indicate otherwise. To further address this issue, rgp120 binding to α-hydroxy galactosylceramide (α-GalCer) was examined. The results are presented in Table 1. As with GalCer, a strong binding event is observed at low protein concentrations with an association constant of $K_a = 3.1 \times 10^8$ M^{-1}, although this value is 5-fold less than the K_a of 1.6×10^9 M^{-1} measured for GalCer (see Table 1). At rgp120 concentrations greater than 25 nM, the binding behavior of GalCer and α-GalCer is quite similar. The recovered K_a and Γ values of 4.6×10^6 M^{-1} and 5.0×10^{-14} mol/cm^2 for α-GalCer are only slightly lower than the corresponding values of 7.5×10^6 M^{-1} and 5.7×10^{-14} mol/cm^2 for GalCer, respectively (Table 1). In summary, these data clearly show that the affinity of rgp120 for galactosylceramides is not significantly affected by α-hydroxylation of the fatty acid chain.

Effect of Phase Segregation on Rgp120 Binding. In addition to the chemical structure of the carbohydrate, the binding of gp120 to GalCer may be influenced by the extent of phase segregation of the lipid bilayer (i.e., the formation of domains enriched in the GSL). This hypothesis has been suggested by Long et al.,[14] based on differences observed in rgp120 binding

(40) Claes, P.; Dunford, M.; Kenney, A.; Vardy, P. In *Laser Light Scattering in Biochemistry*; Harding, S. E., Satelle, D. B., Bloomfield, V. A., Eds.; Royal Society of Chemistry: Cambridge, U.K., 1992; pp 66−67.

(41) TIRF measurements on near monolayer films of albumin and streptavidin in our laboratory consistently yield surface coverages that are 5−10% of a monolayer. An inaccurate estimate for protein film thickness could cause the surface coverage to be either underestimated or overestimated. However, even a highly inaccurate estimate of film thickness (e.g., different from the actual film thickness by 100%) would account for only a minor portion of this error. Energy transfer quenching would yield an underestimated surface coverage, although given typical values for hydrodynamic protein radii and dye:protein labeling ratios, it should not be a predominate source of error. Consequently, the contribution of scattered excited fluorescence to the total measured signal is likely to be the predominate source of the systematic error.

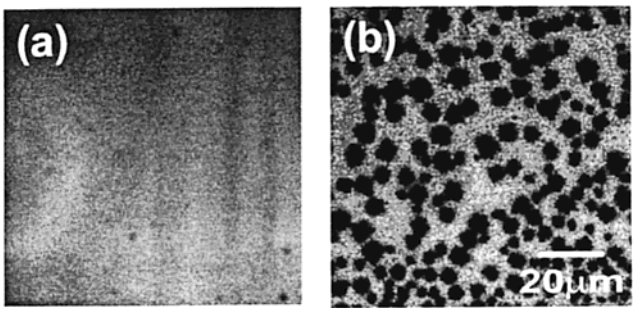

Figure 5. Epifluorescence micrographs of (a) 5 mol % GalCer in POPC monolayer and (b) 50 mol % GalCer in POPC monolayer. Films were deposited by the Langmuir−Blodgett method on fused silica substrates. DOPE labeled with FITC was added (at 0.1 mol %) to visualize phase segregation in the lipid monolayer. The dark areas in (b) represent gel-phase domains of GalCer which have phase-segregated from the liquid-crystalline POPC matrix, in which the FITC-DOPE is preferentially solvated.

as a function of the mole fraction of GalCer in POPC liposomes. Phase segregation of GalCer in a 1-stearoyl-2-oleoyl-*sn*-glycero-3-phosphocholine (SOPC) matrix has been investigated in detail using NMR.[42−45] Above a mole fraction of 0.1, a GalCer-rich gel phase and a liquid-crystalline SOPC-rich phase coexist, which is primarily due to the disparity in the transition temperatures (T_m) for GalCer and SOPC (∼80 and 6 °C, respectively). There is a similar disparity in T_m between GalCer and the matrix lipid POPC ($T_m \approx -2$ °C) used herein and by Long et al.[14] We therefore investigated the effect of GalCer phase segregation on rgp120 binding.

To verify the existence of phase-segregated domains for GalCer/POPC binary mixtures, epifluorescence microscopy was used to image Langmuir−Blodgett monolayers deposited on fused silica slides. To visualize domain formation, a fluorescent probe, FITC-labeled phosphatidylethanolamine (FITC-DOPE), was introduced at 0.1 mol %. At 5 mol % GalCer/95 mol % POPC, the film exhibits uniform fluorescence emission, indicating that the probe is uniformly distributed at optical resolution (Figure 5a). However, at 50 mol % GalCer/50 mol % POPC, the existence of discrete domains is clearly evident (Figure 5b). The FITC-PE is soluble in the liquid-crystalline phase of the lipid monolayer. The dark regions, which are approximately 5 μm in diameter and roughly circular in shape, are solidlike domains of high GalCer concentration, while the lighter areas correspond to fluidlike regions composed predominately of POPC.

Isotherms for rgp120 binding to 5 and 50 mol % GalCer lipid bilayers were measured in the low concentration regime (<20 nM). The binding constants recovered using a Langmuir model were statistically equivalent ($K_a = 1.6 \pm 0.9 \times 10^9$ M^{-1} for 5 mol % and $2.1 \pm 1.3 \times 10^9$ M^{-1} for 50 mol %). These results clearly show that the binding affinity of rgp120 to GalCer is not dependent on the formation of large GalCer domains (i.e., optically resolvable) within the PSLB. Given the statistically equivalent K_a values, further studies of the effect of GalCer concentration on rgp120 binding were not pursued. However, it is important to note that these data and prior studies do not eliminate the possibility that much smaller GSL domains (i.e., smaller than the optical diffraction limit) are present at GSL mole fractions <0.1. If present, such microdomains could faciliate multivalent, high affinity rgp120 binding.

Binding of Rgp120 to Synthetic GSLs. The various GSLs used above were natural isolates and therefore contained a mixture of various fatty acid chain lengths. By synthesizing galactosylceramides with defined chain lengths, we hoped to address the rgp120−GalCer binding event in more detail. We hypothesized that a longer fatty acid chain may make the galactosyl group on GalCer more accessible to rgp120 by projecting the carbohydrate further from the bilayer surface. In the natural mixtures of GalCer used in the TIRF assay, the predominant fatty acid chain lengths were C_{18} and C_{24},[27] whereas the fatty acid chains in POPC are C_{16} and C_{18}. Based on an extended all-trans hydrocarbon chain, there is an ca. 7.5 Å difference in the projection of the carbohydrate above the lipid bilayer surface for the C_{24} versus that of the C_{18} fatty acid chain length of GalCer.

Two synthetic analogues of GalCer, GalCer-C_{18} (**20**), and GalCer-C_{24} (**21**) were prepared according to Scheme 2. The corresponding analogues of α-hydroxy GalCer, α-GalCer-C_{18} (**7a**), and α-GalCer-C_{24} (**7b**) were prepared according to Scheme 1. The chain lengths of these analogues, steroyl (C_{18}) and tetracosanoyl (C_{24}), were chosen because they are the two predominant chain lengths in the natural GalCer mixture.[27]

All four compounds were incorporated into PSLBs and screened for their binding affinity to rgp120 in the low concentration regime (<20 nM). The results are presented in Table 1. The GalCer-C_{18} and GalCer-C_{24} derivatives have binding affinities for rgp120 of 1.2×10^9 and 1.1×10^9 M^{-1} respectively, which are equivalent to the K_a measured for the natural GalCer isolate (**1**). In addition, the saturation surface coverages measured for these two derivatives were comparable to those measured for the natural mixture: 0.20×10^{-14} mol/cm^2 for GalCer-C_{18} and 0.14×10^{-14} mol/cm^2 for GalCer-C_{24}. The K_a values for the α-hydroxylated analogues, α-GalCer-C_{18} and α-GalCer-C_{24}, were 0.37×10^9 and 0.28×10^9 M^{-1}, respectively. These values are equivalent to the K_a measured for the natural α-GalCer isolate (**6**).

Thus for the compounds examined here, the length of the fatty acid chain of GalCer appears to have little influence on the binding of rgp120 when the carbohydrate is presented at the surface of a POPC PSLB. This finding is supported by NMR studies of GalCers of various chain lengths in liposomes in which no direct effect on the presentation or orientation of the terminal carbohydrate group was demonstrated.[46] Furthermore, the effect of α-hydroxylation is identical to that observed when the natural isolates GalCer and α-GalCer were compared (see Table 1). Since the results for the synthetic analogues were equivalent to those obtained with the natural isolates in the low rgp120 concentration regime, binding studies at higher protein concentrations were not pursued.

Conclusions

The results presented here represent the first quantitative measurements of the complex binding process between rgp120

(42) Morrow, M. R.; Singh, D.; Grant, C. W. M. *Biochim. Biophys. Acta* **1995**, *1235*, 239−248.
(43) Morrow, M. R.; Singh, D.; Lu, D. L.; Grant, C. W. M. *Biophys. J.* **1993**, *64*, 654−664.
(44) Morrow, M. R.; Singh, D.; Lu, D.; Grant, C. W. M. *Biochim. Biophys. Acta* **1992**, *1106*, 85−93.
(45) Lu, D. L.; Singh, D.; Morrow, M. R.; Grant, C. W. M. *Biochemistry* **1993**, *32*, 290−297.
(46) Morrow, M. R.; Singh, D. M.; Grant, C. W. M. *Biophys. J.* **1995**, *69*, 955−964.

and GSL receptors at a model lipid membrane surface. The TIRF results clearly demonstrate that a carbohydrate on ceramide is a requirement for rgp120 recognition.

In the low rgp120 concentration regime (<20 nM), GalCer is the preferred receptor, with an affinity constant of ca. 10^9 M^{-1}, which is at the upper range of measured protein−receptor interactions at membrane surfaces. The strength of this binding interaction is comparable to that found for gp120 binding to the surface cell receptor CD4.[39] At higher protein concentrations (25−220 nM), the chemical structure of the carbohydrate plays less of a role. In this regime, rgp120 binds to PSLBs doped with 5 mol % GalCer, LacCer, or GlcCer with an affinity constant of ca. 10^6 M^{-1}. Protein surface coverage measurements are consistent with the binding affinity measurements and show that the high affinity GalCer recognition event observed at low rgp120 concentrations involves only a small fraction of the total number of binding sites. For all three GSLs, the isotherm data suggest that the rgp120 binding process is cooperative, possibly due to GSL aggregation and/or protein−protein interactions at the membrane surface.

The predominate selectivity mechanism for rgp120 to the class of GSL examined here appears to be the chemical structure of the sugar group on ceramide. There is little dependence on the chemical composition of the fatty acid chain of ceramide, in terms of both hydroxylation and fatty acid chain length. Furthermore, formation of gel-phase GalCer domains in fluid lipid bilayer does not affect rgp120 binding affinity at low protein concentrations. In closing, we emphasize that the quantitative results presented here cannot be obtained from ELISA and other nonequilibrium-based techniques. However, our TIRF measurements do complement and, in some cases, substantiate many of the results obtained in previous studies. Finally, the results of this work should aid efforts to design anti-HIV-1 agents based on membrane-tethered, carbohydrate-based receptors for rgp120.

Acknowledgment. Financial support for this research was received from NIH (AI40359-02), NSF (CHE-9726132 and CHE-9623583), Eli Lilly (J.G.H.), and the Alfred P. Sloan Foundation (J.G.H.). J.C.C. was supported as a NRSA fellow under NIH grant F32 GM19914. K.D.M. gratefully acknowledges receipt of the University of Arizona Dean's Fellowship and the Department of Chemistry Carl S. Marvel Fellowship.

Supporting Information Available: Detailed synthetic schemes and characterization data for **7a**, **7b**, **20**, and **21** (PDF). This material is available free of charge via the Internet at http://pubs.acs.org.

JA011225S